Triaxiality and the aligned $h_{11/2}$ neutron orbitals in neutron-rich Zr and Mo isotopes

H. Hua, C. Y. Wu, D. Cline, A. B. Hayes, and R. Teng
Nuclear Structure Research Laboratory, Department of Physics, University of Rochester, Rochester, New York 14627, USA

R. M. Clark, P. Fallon, A. Goergen, A. O. Macchiavelli, and K. Vetter
Nuclear Science Division, Lawrence Berkeley National Laboratory, Berkeley, California 94720, USA
(Received 6 October 2003; published 30 January 2004)

Neutron-rich Zr and Mo isotopes were populated as fission fragments produced by the ^{238}U(α, f) fusion-fission reaction. The level schemes of these nuclei have been extended beyond the first band crossing region, which can be ascribed to the $h_{11/2}$ neutron pair alignment. The spin alignment and signature splitting for the $\nu h_{11/2}$ orbitals in term of triaxiality is addressed. The crossing frequency of the aligned bands in even Zr and Mo isotopes can be reproduced well by calculations using the cranked shell model. Compared to the Zr isotopes, band crossings in Mo isotopes shift to a lower rotational frequency due to the emerging importance of the γ degree of freedom. Within the framework of particle-rotor model, the difference in the signature splitting observed for the $\nu h_{11/2}$ bands between the odd Zr and Mo isotopes can be attributed to the triaxial degree of freedom in the Mo isotopes. The surprising shift of the band crossing to a higher rotational frequency in ^{106}Mo is interpreted as a manifestation of the deformed subshell closure at $N=64$.

DOI: 10.1103/PhysRevC.69.014317 PACS number(s): 23.20.Lv, 25.70.Jj, 27.60.+j

I. INTRODUCTION

For neutron-rich $A\sim100$ nuclei, the valence nucleons begin to fill the $h_{11/2}$ neutron and $g_{9/2}$ proton orbitals. The nuclear structure in this mass region is very sensitive to the occupancy level of these single-particle configurations, which is illustrated by the rapid changes in nuclear spectroscopic properties as a function of both neutron and proton numbers. Manifestations are the sudden onset of quadrupole deformation in the Sr and Zr isotopes, the emerging γ degree of freedom in the Mo-Ru region, and the predicted prolate-to-oblate shape transition in the Pd isotopes. The diverse phenomena of nuclear structure in these nuclei make them an ideal testing ground for various theoretical models [1–3].

Since the neutron-rich $A\sim100$ nuclei lie far from the β stability, the identification of prompt γ rays from fission fragments produced by fission is the main avenue to study nuclear structure of these nuclei. The first such experiment [4] was made by detecting the deexcitation γ rays with a NaI detector in coincidence with the detection of both fission fragments, from a ^{252}Cf fission source, using a pair of solid-state detectors. Subsequently, the improvement in the resolving power of detected γ rays led to the identification of interesting new phenomena. For example, the sudden onset of quadrupole deformation between $N=58$ and 60 was observed in Sr and Zr nuclei [5], which is associated with the competition between the spherical shell gaps and the deformed subshell closure in the single-particle spectrum. The lowest-mass example of identical bands known in two neighboring even-even nuclei was found in ^{98}Sr and ^{100}Sr [6,7]. Other discoveries also include the unusual low-lying excited 0^+ states in ^{98}Sr and ^{100}Zr, which are interpreted as the evidence for shape coexistence [8–10], and the evidence for the emerging triaxial degree of freedom in the Mo-Ru isotopes [11,12].

Significant advances in the study of these neutron-rich nuclei have been made with the advent of large and efficient γ-ray multidetector arrays, Gammasphere and Euroball. One example is the γ degree of freedom in the Mo isotopes, which is manifest by the observation of a spin-dependent triaxial deformation [13] and a harmonic two-phonon γ-vibrational motion [14,15]. While the yrast bands of the Zr and Mo isotopes were extended to higher-spin states, the yrast states of the Ru and Pd isotopes were extended to the band crossing regions for the first time [7], providing an opportunity to study the interplay between single-particle and the collective degrees of freedom. At the same time, theoretical studies of the nuclear structure properties, not only for the ground states [1–3] but also for the high-spin states [2], have been made to try to understand systematically the microscopic origin of rich phenomena mentioned earlier. Even though these nuclei had been studied extensively, a comprehensive understanding of the nuclear structure aspect has not been made, especially, in the high-spin region.

Most of the previous experiments were performed using a source or target sufficiently thick to stop the recoiling fission fragments in order to avoid the Doppler broadening effect for the observed γ rays and to maximize the resulting energy resolution and resolving power for the very dense γ-ray transitions from hundreds of fission fragments. The disadvantage of this approach is that simplification of the complex γ-ray spectrum cannot be made, and the origin of the γ rays from either fission fragment cannot easily be established without relying on the systematics of the γ-ray coincidence relationship between the nucleus of interest and partner nuclei. In addition, it has been established that these neutron-rich nuclei have very significant quadrupole deformation with the deformation parameter β ranging from 0.3 to 0.4, derived from the lifetime measurements. This results in higher-spin states having lifetimes on the order of the stopping times in the target of the recoiling excited nuclei, leading to an appreciable Doppler broadening, which suppresses the observation of the higher-spin transitions.

An alternative approach to the thick-target technique is the coupling of the techniques of coincident fission-product detection with the detection of high-fold γ rays using a source or target on a thin backing. By detecting the fission products, which recoil freely into vacuum, reconstruction of the fission kinematics, such as the determination of masses and velocity vectors for both fission fragments, can be made [16,17]. This allows Doppler-shift corrections to be applied to the observed γ rays, which eliminates the limitation to the study of excited states with lifetimes longer than the stopping times of the fission fragments, imposed by the thick-source or thick-target experiments. This, plus the ability to establish the identities of γ rays originating from either fission fragment, significantly improves the sensitivity for studies of neutron-rich nuclei. For example, in our earlier work using a ^{252}Cf spontaneous fission source [17] and the ^{238}U(α, f) fusion-fission reaction [18] (both the source and the target on a thin backing), the ground-state band of ^{104}Mo was extended from spin 14^+ at 4.114 MeV to spin 20^+ at 7.282 MeV and the $K^\pi = 2^+$, γ-vibrational band from spin 10^+ at 3.004 MeV to spin 16^+ at 5.591 MeV. The yrast sequences of the ^{112}Ru and ^{116}Pd have been extended beyond the second band crossing region which provided evidence of a possible transition of triaxial shape from prolate to oblate occurring in these nuclei [18].

Here we present the results of a systematic study of the high-spin states in neutron-rich Zr and Mo isotopes, which were populated by the ^{238}U(α, f) fusion-fission reaction using the thin-target technique. The level schemes of neutron-rich Zr and Mo isotopes have been extended substantially both in spin and excitation energy. An analysis of the Zr and Mo isotopes in the framework of the cranked shell model (CSM) [19] and the particle-rotor model [20–22] have been performed. Comparison of the experimental data with model calculations confirms that the $h_{11/2}$ neutron alignment is responsible for the first band crossing in Zr isotopes, as well as in Mo isotopes, as described in a previous publication [23]. This study supports the conclusion that the triaxial degree of freedom plays an important role in the Mo isotopes while the Zr isotopes still have a more axially symmetry shape. The deformed subshell closure at $N=64$ is manifest by the observed delayed $h_{11/2}$ neutron crossing in ^{106}Mo. Some of these results have been reported in Refs. [24,25].

II. EXPERIMENT

The present experiment was performed at the 88-in. cyclotron facility of the Lawrence Berkeley National Laboratory by bombarding a ^{238}U target with an α beam at $E_{\rm lab} = 30$ MeV. Neutron-rich Zr and Mo isotopes were populated as fission fragments produced by the ^{238}U(α, f) fusion-fission reaction. A 300 μg/cm^2 ^{238}U target on a $\approx$30 μg/cm^2 thickness carbon backing was used, allowing the fission fragments to recoil out of the thin target into vacuum and to be detected. The Rochester 4π, highly segmented heavy-ion detector array CHICO [26] was used to detect the fission fragments in coincidence with the detection of at least three de-excitation γ rays using Gammasphere. CHICO is an ideal detector for such study since it is insensitive to light ions, such as α particles, and it has long-term stability under high counting rate. This detector has a geometric coverage for scattering angles from 12° to 85° and 95° to 168° relative to the beam axis and an azimuthal angle totaling 280° out of 360°. A valid event required the detection of both fission fragments and coincident γ rays. The fission fragment scattering angles, and their time-of-flight difference, were recorded in addition to the γ-ray energies and coincident time. A total of $\approx 6 \times 10^8$ p-p-γ-γ-γ events were collected.

The masses and velocity vectors of the fission fragments were deduced from the measured angles of both fission fragments and their time-of-flight difference, assuming the total kinetic energy is the same as that for ^{240}Pu spontaneous fission [27]. This assumption, that the prompt fission originates from the Pu-like compound nucleus, was supported by the observed γ-ray cross correlation between the partner fragment pairs. The deduced mass distribution of the fission fragments, shown in Fig. 1, has a mass resolution of 12 mass units, which reflects the time resolution, $\approx$500 ps, plus the achieved position resolution of $\approx$1° in polar angle and 4.6° in azimuthal angle. The obtained resolutions are consistent with prior CHICO performance [16,28–31].

To increase the sensitivity in channel selection, mass-gated events with three or higher γ rays were used to develop the level schemes of Zr and Mo isotopes. The additional selectivity of mass reduces the γ-ray "background" of nuclei that are not of current interest, which enhances the ability to study nuclei produced with low yield or having weak transition strengths. Doppler-shift corrected γ-ray spectra gated by the mass and the known γ-ray transitions in ^{100,101}Zr are shown in Fig. 2. The resulting energy resolution is better than 1%, limited primarily by the finite size of Ge detector. Since the origin of γ rays from either fission fragment was established, after the proper Doppler-shift corrections were made, no sharp γ-ray transitions from the partner Xe isotopes are visible in these spectra. Thus the resultant spectra are clean and straightforward to interpret.

III. RESULTS AND DISCUSSION

A. Zr isotopes

Partial level schemes of the neutron-rich ^{100,102,104}Zr deduced from the present work are shown in Figs. 3–5, respectively. The ground-state bands of these Zr isotopes were previously established up to spins of 14^+, 12^+, and 8^+, respectively, by Hotchkis *et al.* [32] and Hamilton *et al.* [7], using spontaneous fission sources of ^{248}Cm and ^{252}Cf with a thick backing. In the present work, the ground-state bands of ^{100,102,104}Zr were extended to spin 20^+ at 7.615 MeV, 20^+ at 7.452 MeV, and 14^+ at 4.224 MeV, respectively.

The level schemes of the neutron-rich ^{101,103}Zr derived from this work are shown in Figs. 6 and 7, respectively. Lower-spin members of the ground-state bands in ^{101,103}Zr, which have different single-particle configurations, have been reported earlier [7,32]. The rotational band built on the 216.8 keV state in ^{101}Zr is assigned to have the same single-particle configuration as the ground-state band in ^{103}Zr. All these bands have been extended substantially by the present work. For ^{101}Zr, the $3/2^+[411]$ (ground-state) band has been

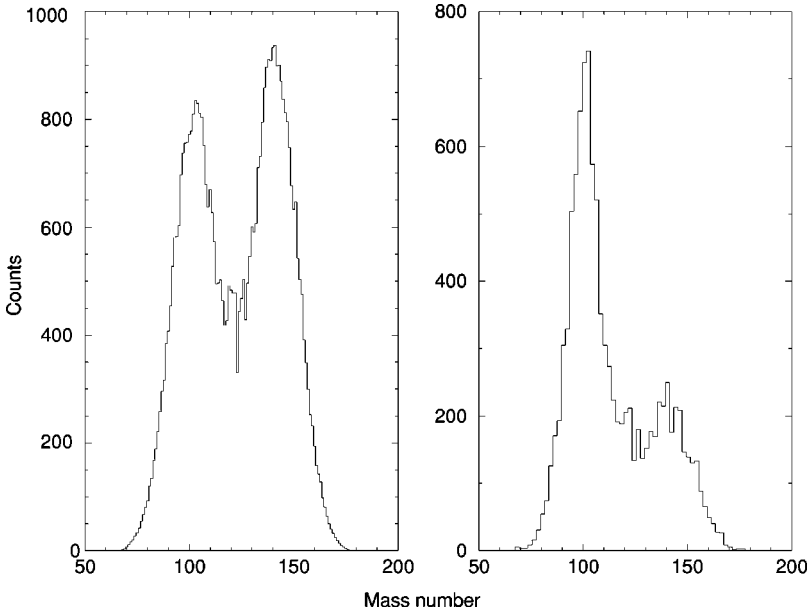

FIG. 1. The fission-fragment mass distribution deduced from ^{238}U(α, f) fusion-fission reaction (left) and with the gates on the $2^+ \rightarrow 0^+$ and $4^+ \rightarrow 2^+$ transitions of ^{100}Zr (right).

extended from spin $23/2^+$ at 2.489 MeV to spin $39/2^+$ at 6.507 MeV, while the $5/2^-[532]$ band was extended from spin $23/2^-$ at 2.330 MeV to spin $39/2^-$ at 6.412 MeV. For ^{103}Zr, the $5/2^-[532]$ (ground-state) band has been extended from spin $19/2^-$ at 1.473 MeV to spin $31/2^-$ at 4.028 MeV.

The high-spin states, extended by the present work, in the neutron-rich Zr nuclei allow study of the band crossing phenomena in these nuclei. Plots of the moments of inertia for the rotational bands in ^{100,102,104}Zr and in ^{101,103}Zr as a function of rotational frequency are shown in Figs. 8 and 9, respectively. An upbending behavior is observed for the ground-state bands of ^{100,102,104}Zr as well as for the $3/2^+[411]$ band in ^{101}Zr in these plots. The observed blocking effects for the $h_{11/2}$ orbitals ($5/2^-[532]$ band) in ^{101,103}Zr and the evidence of no blocking for the spin alignment of the $d_{5/2}$ orbitals ($3/2^+[411]$ band) in ^{101}Zr suggest that the band crossings for the ground-state bands of ^{100,102}Zr can be ascribed to the alignment of a $h_{11/2}$ neutron pair. This is further supported by the gain in the spin alignment of $\approx 10\hbar$, similar for both ^{100}Zr and ^{102}Zr, using the Harris parameters $\mathcal{J}_0 = 3\hbar^2/\mathrm{MeV}$ and $\mathcal{J}_1 = 30\hbar^4/\mathrm{MeV}^3$.

The band crossing phenomena in ^{100,102}Zr have been studied using the cranked shell model by Skalski *et al.* [2]. The observed gain in the spin alignments for these nuclei is well reproduced by the calculations assuming the first band crossing is caused by the aligned $h_{11/2}$ neutron orbitals, but the calculated crossing frequency ≈ 350 keV for ^{102}Zr is ≈ 140 keV lower than the experimental value, ≈ 490 keV. Our CSM calculations using a Woods-Saxon potential [19] for ^{102}Zr are presented in Fig. 10, where the quadrupole deformation parameter $\beta \approx 0.39$ was derived from the lifetime measurement [33] and an axially symmetric shape ($\gamma = 0°$) was assumed. The predicted band crossing due to the $h_{11/2}$ neutron alignment at the rotational frequency ≈ 500 keV is considerably lower than that of the $g_{9/2}$ proton alignment and is very close to the experimental value for ^{102}Zr. Similar

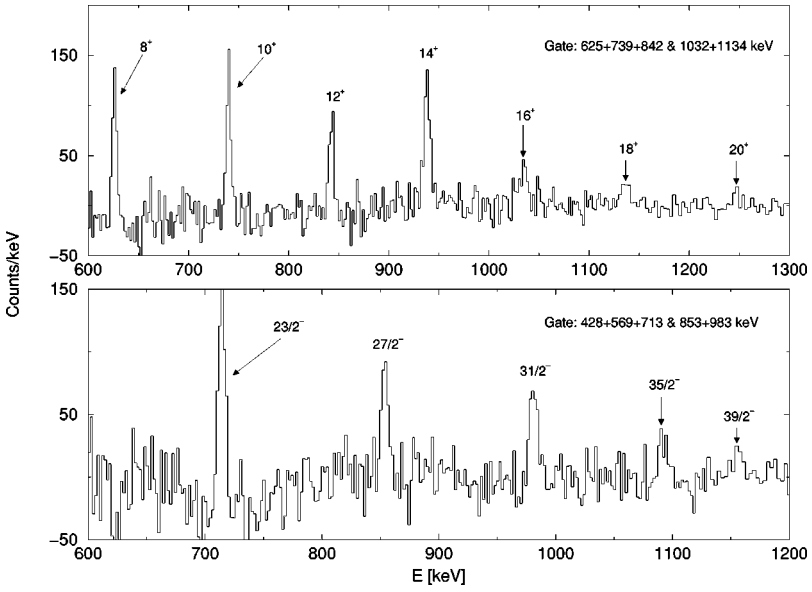

FIG. 2. Doppler-shift corrected spectra with gates on the mass ($90 \leqslant A \leqslant 115$) and known γ-ray transitions in ^{100}Zr (top) and ^{101}Zr (bottom). The labeled transitions are $\Delta I = 2$ transitions.

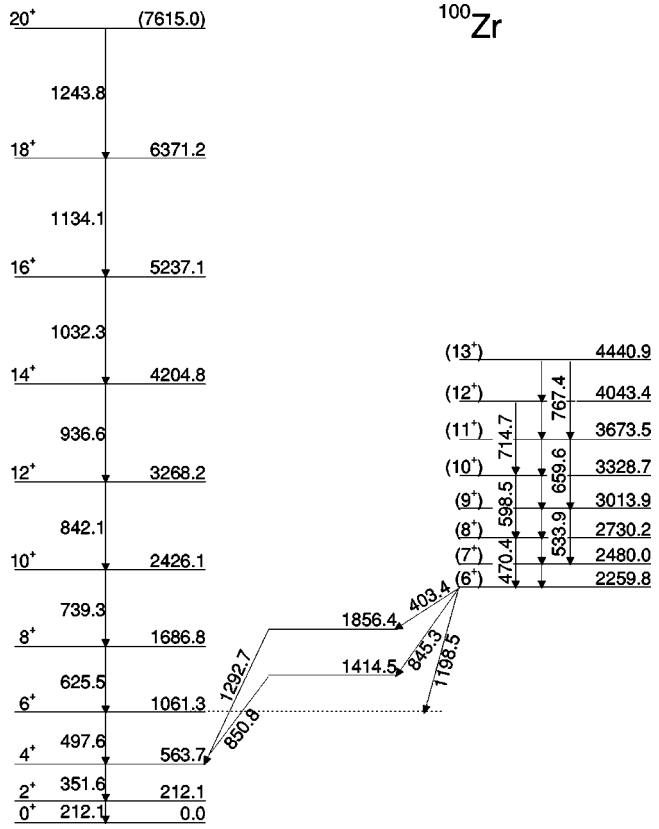

FIG. 3. Partial level scheme of ^{100}Zr. Energies are in keV.

results were also obtained for ^{100}Zr. It supports the interpretation that the alignment of $h_{11/2}$ neutron orbitals is responsible for the first band crossing in the neutron-rich Zr isotopes. The difference in the predicted crossing frequency between our calculations and the ones made by Skalski *et al.* [2] results mainly from the ≈30% stronger pairing strength used in the former, and partly from the different quadrupole deformation parameter used, $\beta=0.39$ in the former compared to 0.30 for the latter.

The rotational band built on the 2259.8 keV state in ^{100}Zr has been established by Durell *et al.* [34,35] and Hamilton *et al.* [36]. Three more new levels were added to this band in the present work. This two-quasiparticle band was assumed to have the $\pi 5/2^+[422]\otimes\pi 5/2^-[303]$ configuration with $K^\pi=5/2^-$ by Hamilton *et al.* [36], while Durell *et al.* [35] assumed it has the $\nu 9/2^+[404]\otimes\nu 3/2^+[411]$ configuration with $K^\pi=6^+$. The $K^\pi=5^-$ state also can be formed by the $\nu 5^-[532]\otimes\nu 5/2^+[413]$ configuration. However, since the $h_{11/2}$ neutron orbitals are involved in the alignment of the ground-state band, a similar alignment observed in this excited band (see Fig. 8) implies that the $\nu 5/2^-[532]$ configuration does not play a role in its wave functions. The rotational band built on either $5/2^+[422]$ or $5/2^-[303]$ proton configuration has been identified in ^{101,103}Nb and ^{99,101}Y nuclei while the rotational band built on the $9/2^+[404]$ neutron configuration has been identified recently in ^{99}Zr [37]. The calculated $|(g_K-g_R)/Q_0|$ value for the $\nu 9/2^+[404]\otimes\nu 3/2^+[411]$ configuration is $0.13(e\ \mathrm{b})^{-1}$ assuming $g_K=-0.255$ [37] and −0.14 [38] for the $9/2^+[404]$ and $3/2^+[411]$ neutron configurations, respectively. The g_K value for the latter configuration is based on the assumption that the first $3/2^+$ state in ^{101,103}Ru is due to the $3/2^+[411]$ neutron configuration. $g_R=0.22$ was taken to be equal to the g factor of the first 2^+ state in ^{100}Zr [38]. The $|(g_K-g_R)/Q_0|$ value for the $\pi 5/2^+[422]\otimes\pi 5/2^-[303]$ configuration was calculated to be $0.16(e\ \mathrm{b})^{-1}$ by Hotchkis *et al.* [32]. Our measured value, $0.12(1)(e\ \mathrm{b})^{-1}$, for the $|(g_K-g_R)/Q_0|$ is consistent with the calculated value of $0.13(e\ \mathrm{b})^{-1}$ for the $\nu 9/2^+[404]\otimes\nu 3/2^+[411]$ configuration which thus favors such an assignment.

Two rotational bands built on two-quasiparticle states, in addition to the ground-state band, were identified in ^{102}Zr. One is the $K^\pi=4^-$ band with the intrinsic excitation energy of 1821.9 keV [34–36] and the other is the possible $K^\pi=5^-$ band, labeled band (a) in Fig. 4, with the intrinsic excitation energy of 1660.1 keV [7]. The $K^\pi=4^-$ band was extended to spin 10^- by the present work and was assumed to have the $\nu 5/2^-[532]\otimes\nu 3/2^+[411]$ configuration by Durell *et al.* [35]. This is supported by the agreement between the calculated

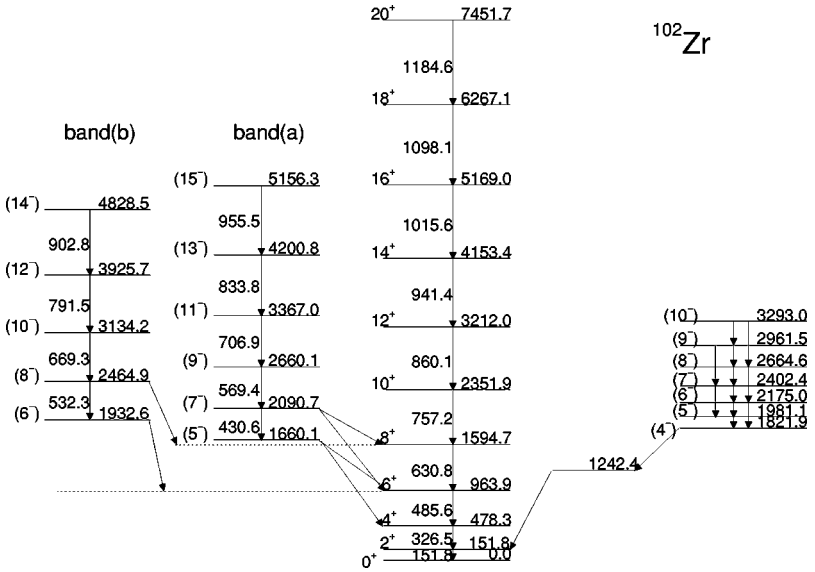

FIG. 4. Partial level scheme of ^{102}Zr. Energies are in keV.

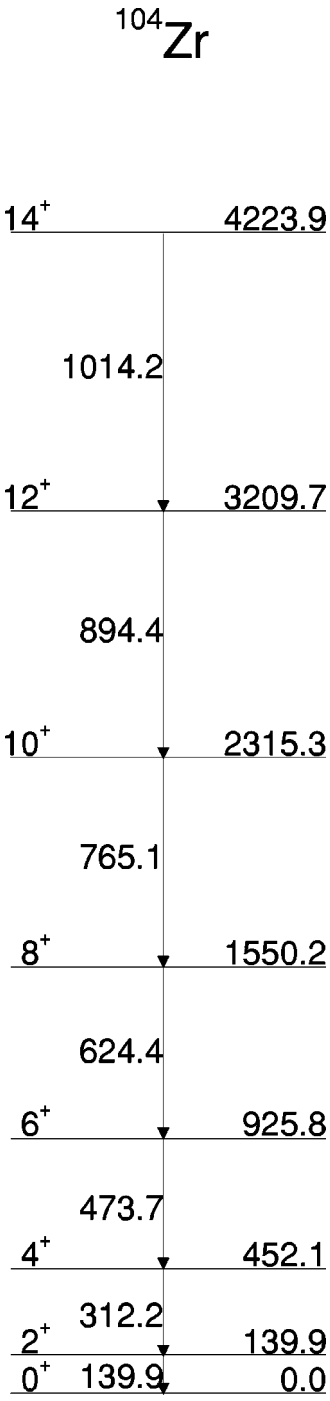

FIG. 5. Partial level scheme of ^{104}Zr. Energies are in keV.

$|(g_K-g_R)/Q_0|$ value, $0.15(2)(e\ \mathrm{b})^{-1}$, and the previously measured value, $0.14(1)(e\ \mathrm{b})^{-1}$ [35]. Both of these values also are in good agreement with our measured ratio of $0.16(1)(e\ \mathrm{b})^{-1}$.

The band (a) in ^{102}Zr, which couples strongly to the ground-state band [7], was extended to spin 15^- at 5.156 MeV by the present work. A new set of coincident γ transitions, 532.3, 669.3, 791.5, and 902.8 keV, was observed by setting a summed gate on the 151.8, 326.5, and 485.6 keV transitions in coincidence with 968.7 keV transition. From the systematics of transition energies, those newly identified γ rays could be the transitions for the unnatural-parity partner states of the band (a), which is labeled as band (b) in Fig. 4. There are three low-lying single-neutron configurations, $5/2^-[532]$, $5/2^+[413]$, and $3/2^+[411]$, that are located within 310 keV of each other in ^{105}Mo [39] and could be relevant to the two-quasiparticle configuration of bands (a) and (b) in ^{102}Zr. The two-quasineutron configuration, $5/2^-[532]\otimes 3/2^+[411]$, has been identified as the underlying single-particle structure for the $K^\pi=4^-$ band at 1821.9 keV in ^{102}Zr as mentioned earlier. The $K^\pi=5^-$ formed by the two-quasineutron configuration, $5/2^-[532]\otimes 5/2^+[413]$, could be the underlying single-particle structure for the bands (a) and (b) with the intrinsic excitation energy of 1660.1 keV. A similar band structure to band (a) was identified in isotone ^{104}Mo, and more discussion of this assigned two-quasineutron configuration is given later.

One common feature among all the rotational bands built on the two-quasiparticle configurations for both even Zr and Mo isotopes is that the kinematic moment of inertia is nearly independent of the rotational frequency and approaches the rigid-rotor limit. This phenomenon is closely related to the weak pairing correlations in these neutron-rich nuclei, which has been addressed by Durell *et al.* [35] based on the observed bandhead excitation energies of rotational bands built on the two-quasineutron excitation in ^{100,102}Zr.

B. Mo isotopes

In the earlier study with a ^{248}Cm source, the ground-state bands in the neutron-rich ^{102,104,106,108}Mo were established up to spins of 8^+, 12^+, 10^+, and 10^+, respectively, as well as the γ-vibrational bands in ^{104,106,108}Mo up to spins of 10^+, 8^+, and 9^+, respectively [14,15,32]. The ground-state bands of these Mo isotopes were further extended to spins of 12^+, 14^+, 14^+, and 12^+, respectively, by the work of Hamilton *et al.* [7] using a ^{252}Cf source. In our earlier work with a thin ^{252}Cf source, these Mo isotopes have been observed up to spin 14^+ at 4.503 MeV, 20^+ at 7.283 MeV, 18^+ at 6.500 MeV, and 16^+ at 5.347 MeV, respectively, for the ground-state bands [17]. The level diagrams for ^{102,104,106,108}Mo based on the present work agree with those previous results and are showed in Figs. 11–14, respectively. One new level was added to each of the ground-state bands in ^{102,106}Mo. The γ-vibrational bands in ^{104,106,108}Mo were extended to spin 18^+ at 6.624 MeV, 18^+ at 6.867 MeV, and 11^+ at 3.338 MeV, respectively. The previously established rotational bands built on the two-phonon γ-vibrational states in ^{104,106}Mo [14,15] were confirmed by the present work. Four new states were added to the two-phonon γ-vibrational band in ^{106}Mo.

The level schemes of the neutron-rich ^{103,105,107}Mo derived from this work are shown in Figs. 15–17, respectively. The yrast sequences of ^{103,105}Mo extended into the band crossing region were reported in our earlier publication [23]. In the present work with four times more statistics compared to our earlier work using the same fusion-fission reaction, the $3/2^+[411]$ (ground-state) band in ^{103}Mo was extended from spin $31/2^+$ at 4.215 MeV to spin $39/2^+$ at 6.309 MeV and the decoupled $5/2^-[532]$ band was extended from spin $35/2^-$ at

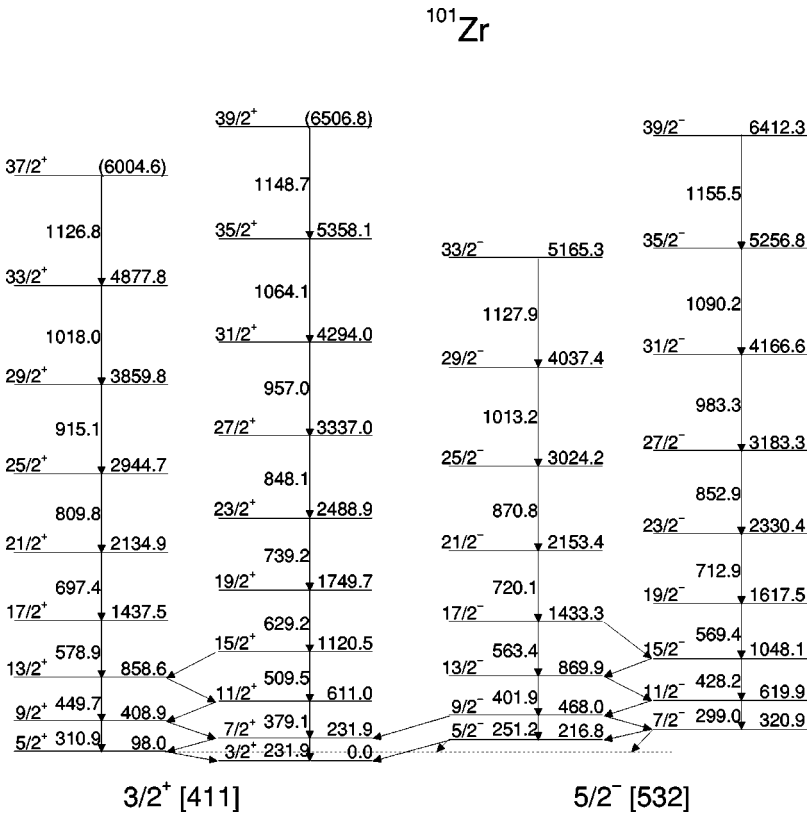

FIG. 6. Partial level scheme of ^{101}Zr. Energies are in keV.

4.983 MeV to spin $39/2^-$ at 6.149 MeV. For ^{105}Mo, two excited states with energies at 246.9 keV and 396.9 keV, respectively, were reported previously in the β decay study of ^{105}Nb. The 246.9 keV level is the favored candidate for the state with the $3/2^+[411]$ configuration suggested by Lhersonneau *et al.* [39] based on the systematic study of the levels in the ^{101}Sr, ^{103}Zr, and ^{105}Mo isotones. This also is assumed by Liang *et al.* [40]. The population of these two excited states were observed in the present work. By requiring the coincidence between the known 246.9 keV and 150.0 keV γ transitions, new coincident γ transitions of 265.4, 415.4, 538.8, and 658.5 keV were observed. The $3/2^+[411]$ band shown in Fig. 16 was constructed by relying on the systematics of energy and intensity of the above coincident γ rays. For the $5/2^-[532]$ (ground-state) band in ^{105}Mo, a correction was made to our earlier report on the excitation energy of the state with spin $33/2^-$. The correct excitation energy is 4743.8 keV.

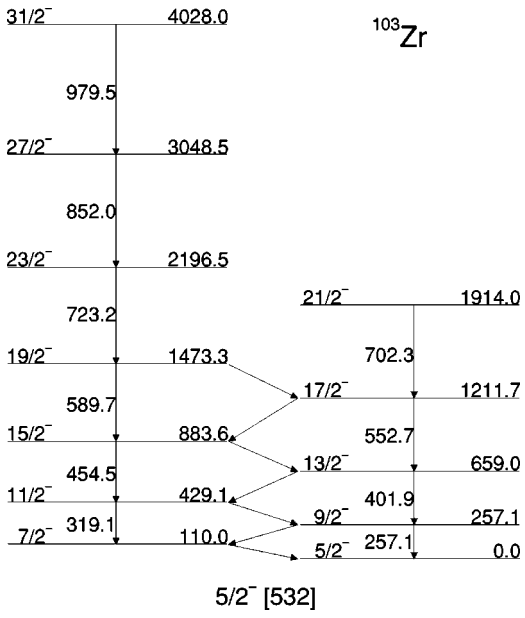

FIG. 7. Partial level scheme of ^{103}Zr. Energies are in keV.

The level scheme of ^{107}Mo is very complex and difficult to interpret. In the earlier study by Hotchkis *et al.* [32], no spin and parity was assigned to the low-lying levels. By determining the total internal conversion coefficients for several low-energy transitions, from the intensity balance in and out of a level, and studying their systematics, Hwang *et al.* [41] have assigned the tentative spins and parities to the levels in ^{107}Mo and grouped them into the ground-state band and the rotational bands built on the $5/2^-[532]$ and $5/2^+[413]$ neutron configurations. In this work, all these rotational bands were observed and extended to higher-spin states. The $5/2^+[413]$ band was extended from spin $19/2^+$ at 1.588 MeV to spin $31/2^+$ at 4.196 MeV and the $5/2^-[532]$ band was extended from spin $23/2^-$ at 2.242 MeV to spin $35/2^-$ at 5.053 MeV. The decoupled (ground-state) band built on the $h_{11/2}$ neutron configuration was extended from spin $23/2^-$ at 1.798 MeV to spin $35/2^-$ at 4.511 MeV.

Plots of the moments of inertia as a function of rotational frequency for the ground-state bands in ^{102,104,106,108}Mo are shown in Fig. 18. Such plots for the rotational bands in ^{103,105,107}Mo are shown in Fig. 19. An upbending behavior was observed in all the ground-state bands of ^{102,104,106,108}Mo and the $3/2^+[411]$ band in ^{103}Mo, which is similar to that of

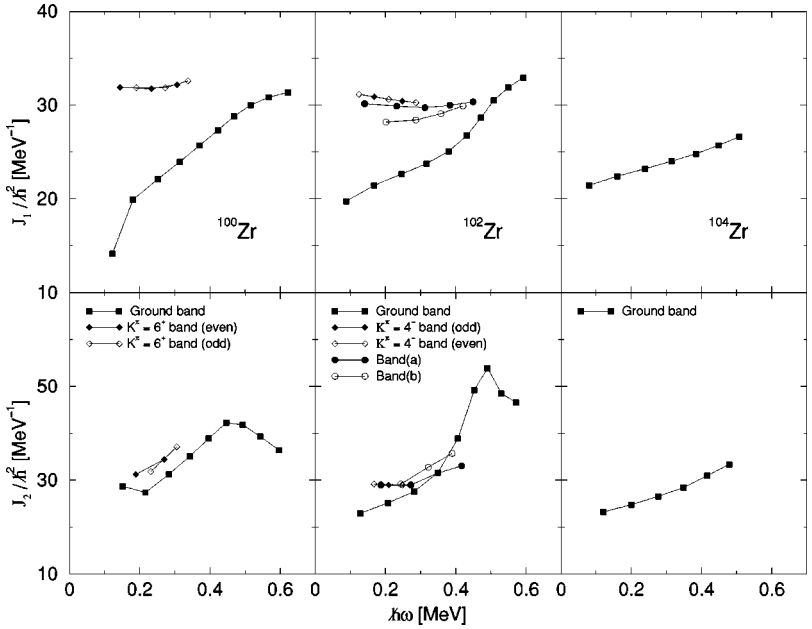

FIG. 8. The kinematic (top) and dynamic (bottom) moments of inertia as a function of the rotational frequency for the rotational bands in ^{100,102,104}Zr.

the Zr isotopes. Beyond the band crossings, the kinematic moments of inertia for ^{102,104,106}Mo are close to each other and approach the rigid-rotor limit. The observed band crossing in ^{103,104}Mo, which has been discussed in our recent publication [23], can be attributed to the alignment of a pair $h_{11/2}$ neutrons based on the observed alignment in the $3/2^+[411]$ band of ^{103}Mo and blocking effect in the $5/2^-[532]$ band of ^{105}Mo. This is further supported by the gains in the spin alignment of $\approx 10\hbar$ for ^{102,104,106}Mo using the Harris parameters $\mathcal{J}_0 = 3\hbar^2/\mathrm{MeV}$ and $\mathcal{J}_1 = 45\hbar^4/\mathrm{MeV}^3$.

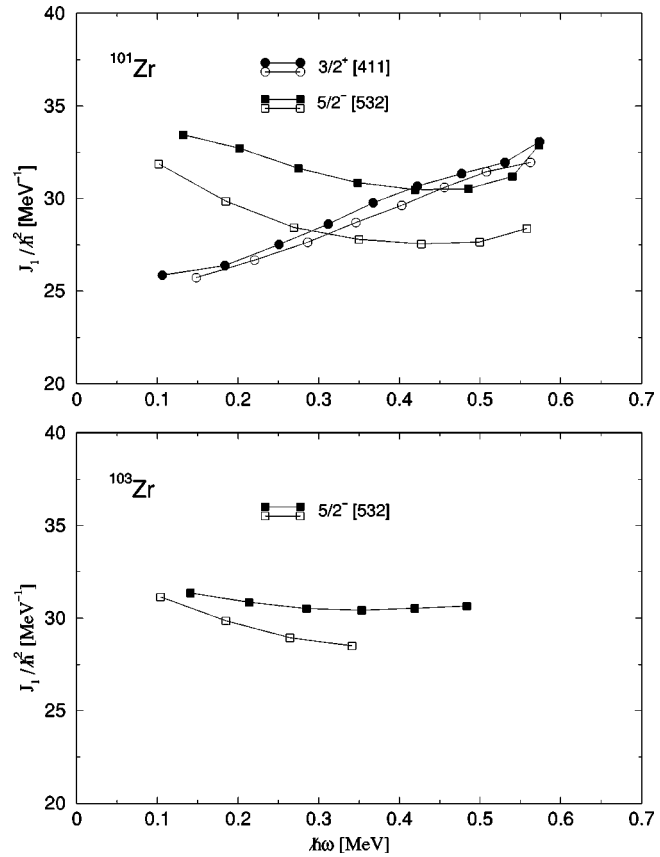

FIG. 9. The kinematic moment of inertia as a function of the rotational frequency for the rotational bands in ^{101}Zr (top) and ^{103}Zr (bottom).

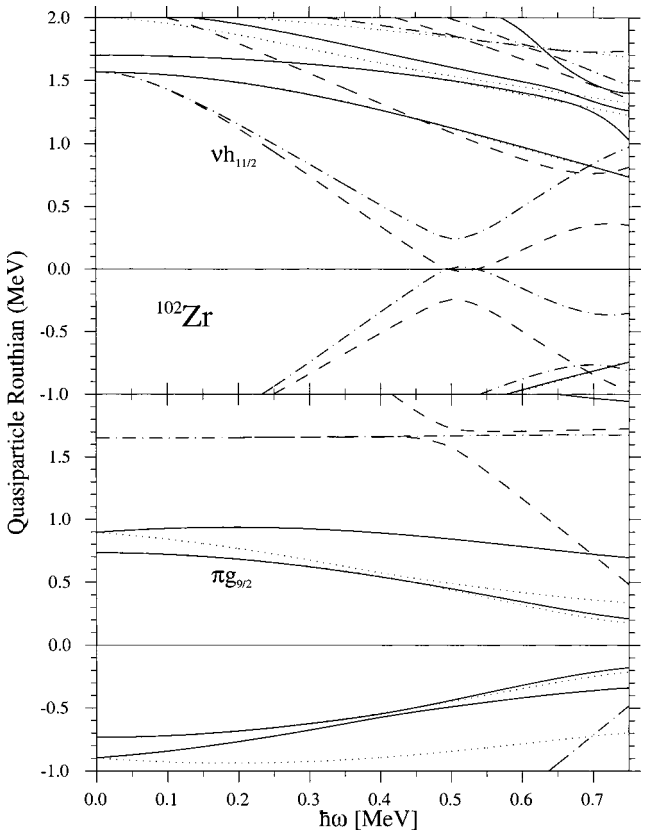

FIG. 10. Cranked shell model calculations for ^{102}Zr. (π, α): solid $=(+, +1/2)$, dotted $=(+, -1/2)$, dash-dotted $=(-, +1/2)$, and dashed $=(-, -1/2)$. The parameters used were $\beta_2 = 0.39$, $\beta_4 = 0.00$, $\gamma = 0°$.

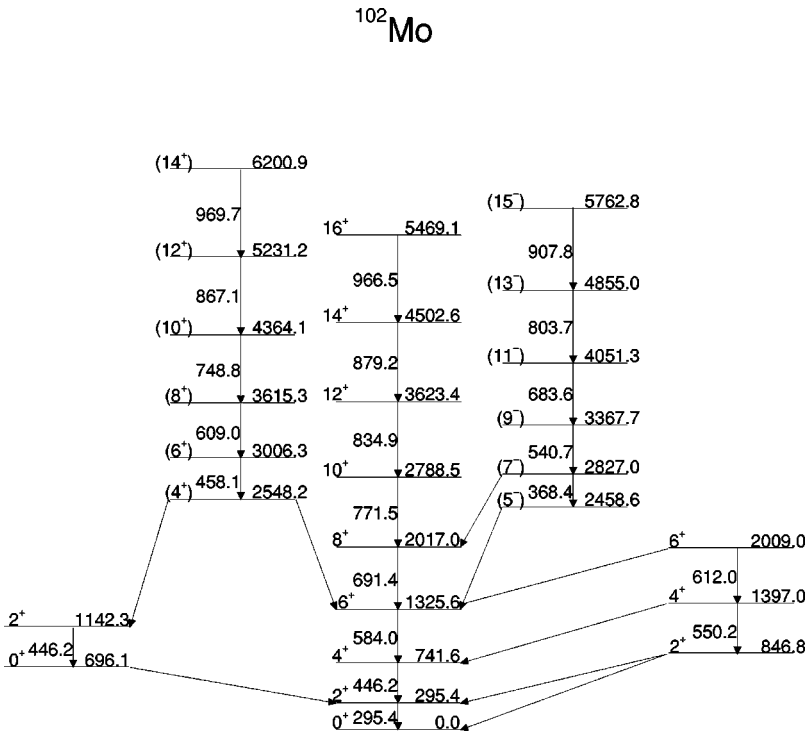

FIG. 11. Partial level scheme of ^{102}Mo. Energies are in keV.

The band crossing phenomenon in the Mo isotopes was studied within the framework of the cranked shell model [19], an example is shown in Fig. 20, where the calculation for ^{104}Mo was made using the quadrupole deformation parameter, $\beta \approx 0.33$ [42], and a triaxial shape with $\gamma = -19°$ [15]. The predicted crossing frequency for the $h_{11/2}$ neutron alignment is significantly lower than that for the $g_{9/2}$ proton alignment and is in reasonable agreement with the observed crossing frequency. It provides a complementary confirmation for the cause of the first band crossings in the neutron-rich Mo isotopes. Introducing the triaxial deformation for the Mo isotopes in the CSM calculations does lower the crossing frequency for the $h_{11/2}$ neutron alignment relative to that for the Zr isotopes despite the fact that they have very similar quadrupole deformation.

According to both the experimental observation and the theoretical calculations [2], ^{104}Mo and ^{106}Mo have very similar quadrupole and γ deformations. Therefore, it is surprising to find that the rate of the spin alignment and the crossing frequency between these two isotopes are quite different,

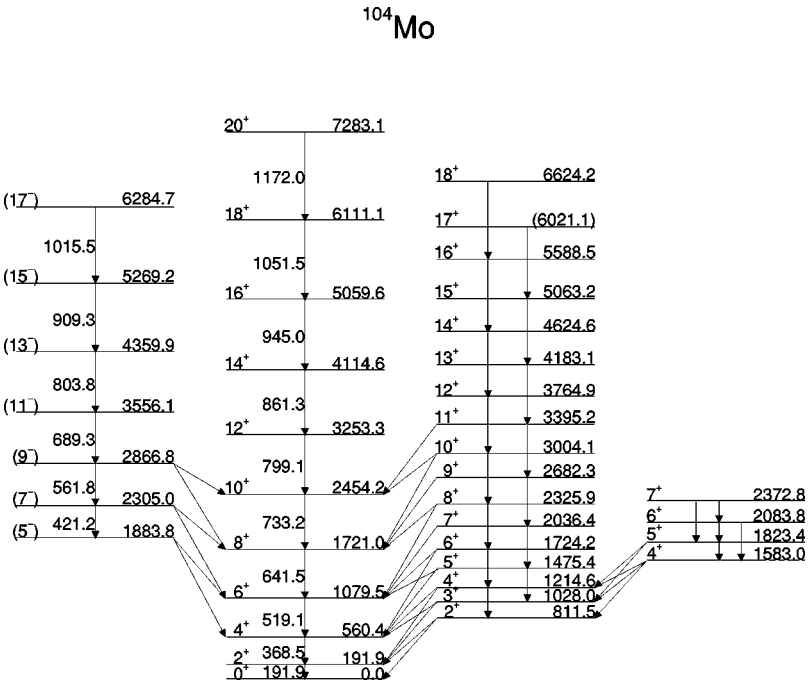

FIG. 12. Partial level scheme of ^{104}Mo. Energies are in keV.

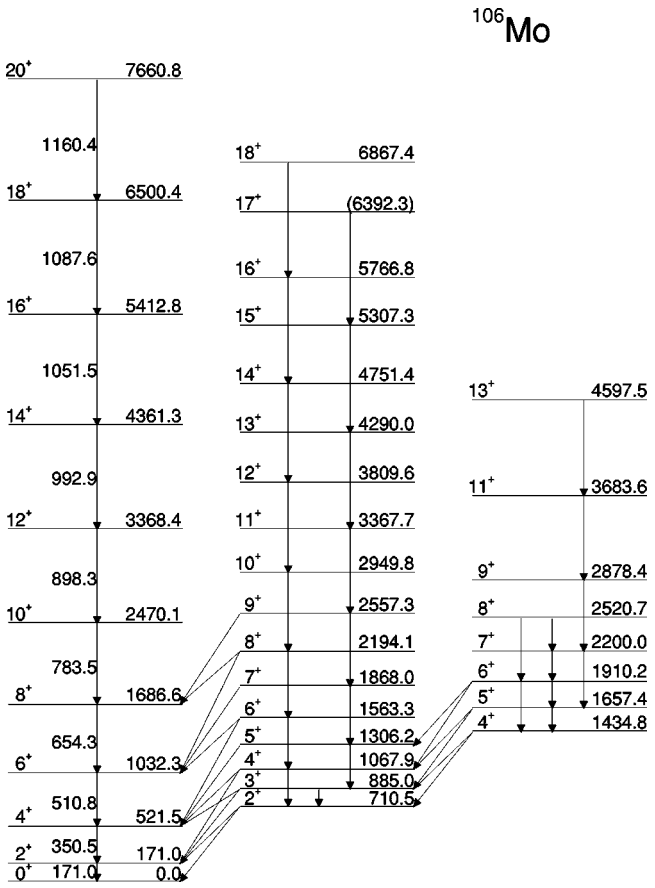

FIG. 13. Partial level scheme of ^{106}Mo. Energies are in keV.

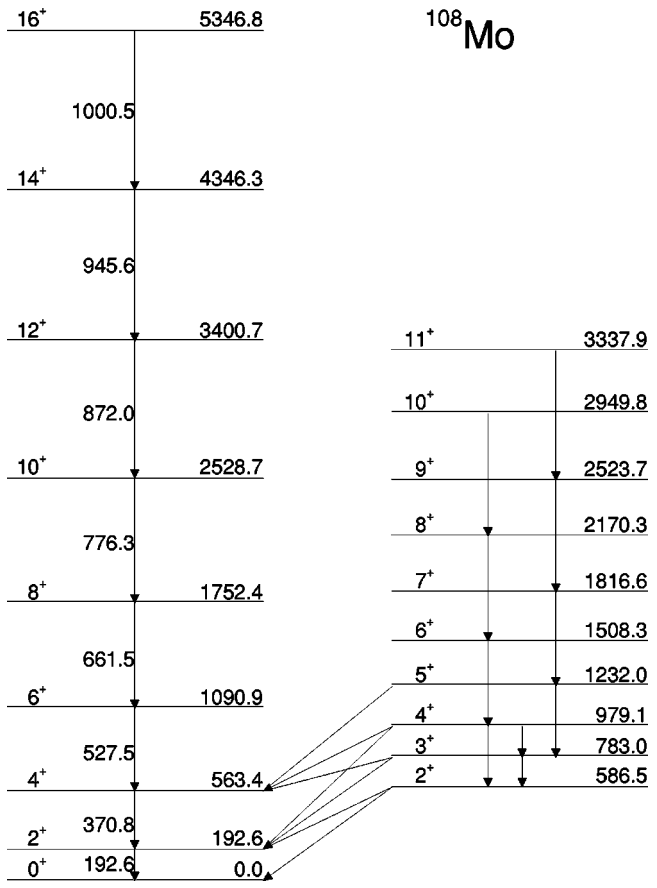

FIG. 14. Partial level scheme of ^{108}Mo. Energies are in keV.

which can be seen in Fig. 18. This disparity in the observed quantities is most likely due to the deformed subshell closure effect at neutron number 64 for ^{106}Mo, which was predicted by Skalski *et al.* [2]. The same calculations predicted that the transitional nucleus ^{102}Mo is very soft and the isotopes ^{104,106,108}Mo have well-defined triaxial ground-state minima. The similarity of the observed J_2 moment between ^{102}Mo and ^{104}Mo indicates that the spin-alignment rate and the crossing frequency are insensitive to the softness of the shape degrees of freedom for a quadrupole deformation.

There is an interesting difference in the moment of inertia for the $5/2^-[532]$ band between the odd Zr and Mo isotopes. The moments of inertia for different signatures cross each other at the rotational frequency $\approx$500 keV for the Mo isotopes, which is shown in Fig. 19 but not in the Zr isotopes (see Fig. 9). This phenomenon was studied under the framework of particle-rotor model [20–22]. The calculations together with the experimental data for ^{101}Zr and ^{103}Mo are shown in Fig. 21, where the signature splitting as a function of spin is plotted. The trend of signature splitting is very sensitive to the γ degree of freedom. Assuming $\gamma=0°$, the calculations reproduce the trends of the data very well for ^{101}Zr but not for ^{103}Mo. Only with appreciable γ deformation values can the calculations reproduce the trends of the experimental data for ^{103}Mo. The difference in the signature splitting for the $5/2^-[532]$ band between the odd Zr and Mo isotopes could be a manifestation of the γ degree of freedom.

Two rotational bands besides the ground-state band were observed in ^{102}Mo for the first time. The rotational band built on the 2548.2 keV state, shown in Fig. 11, was tentatively assigned to have $K^\pi=4^+$ because of the unique decay pattern of its bandhead. It decays not only to the 6^+ state of the ground-state band but also to the 2^+ state of the excited 0^+ band at 696.1 keV. The three close-lying single-neutron configurations $5/2^-[532]$, $5/2^+[413]$, and $3/2^+[411]$, mentioned earlier, could be relevant to the discussion of the underlying two-quasiparticle excitation of this rotational band. The possible two-quasiparticle candidate is the $K^\pi=4^+$ state formed by the two-quasineutron $5/2^+[413]\otimes 3/2^+[411]$ configuration. For the rotational band built on the 2458.6 keV state, the transition energies and the decay pattern to the ground-state band are similar to those of the $K^\pi=5^-$ band in both ^{102}Zr and ^{104}Mo. Therefore, it was tentatively assigned to have $K^\pi=5^-$ with the two-quasineutron $5/2^-[532]\otimes 5/2^+[413]$ configuration. Confirmation of these assignments certainly requires more experimental spectroscopic information and theoretical study.

In ^{104}Mo, the rotational band built on the 1883.8 keV state has been identified earlier [15,43]. Three more levels were added to this band by the present work. The two-quasiproton $5/2^+[422]\otimes 5/2^-[303]$ configuration was suggested to be the underlying single-particle configuration of this rotational band [43]. However, their decay pattern, such as the $\Delta I=1$ intraband transition, is very close to that of band (a) in ^{102}Zr, which was built on the two-quasiparticle excitation with the $\nu 5/2^-[532]\otimes\nu 5/2^+[413]$ configuration. A qualitative measure of the octupole strength in this band was

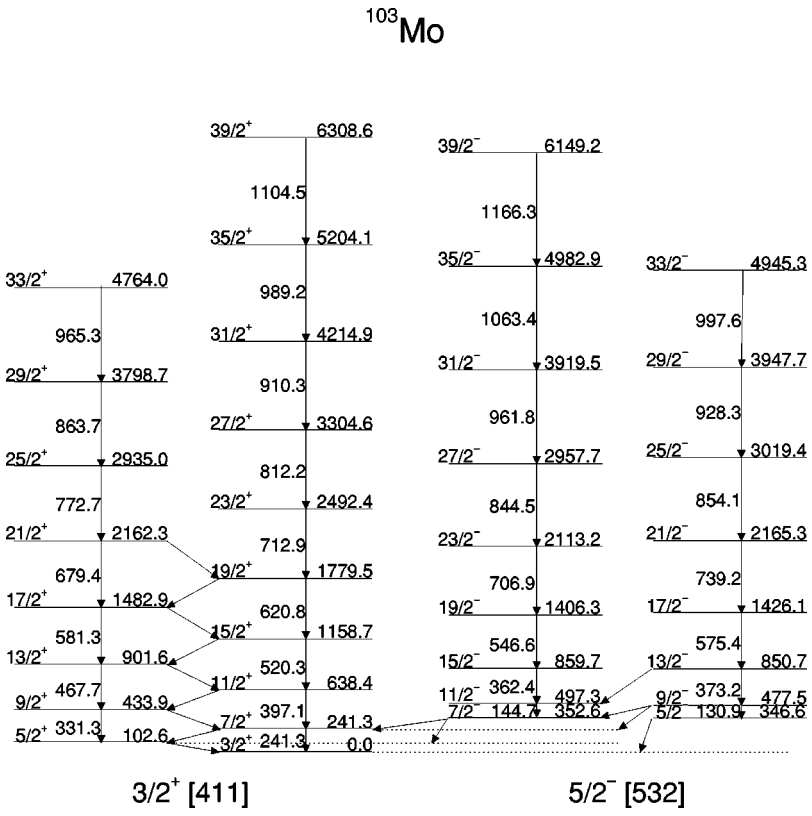

FIG. 15. Partial level scheme of ^{103}Mo. Energies are in keV.

made by measuring the $E1$ strength to the ground-state band. From the intensity ratios between the interband and the intraband transitions in ^{104}Mo, one has a measure of the $E1$ strength from the $B(E1, I^- \rightarrow (I+1)^+)/B(E2, I^- \rightarrow (I-2)^-)$ ratios. This ratio was measured to be $0.14(3) \times 10^{-6}$ fm^{-2} for the $I^\pi = 7^-$ state, which is about an order of magnitude smaller than that for the octupole deformed ^{142,144}Ba isotopes [7,44], indicating weaker octupole correlation.

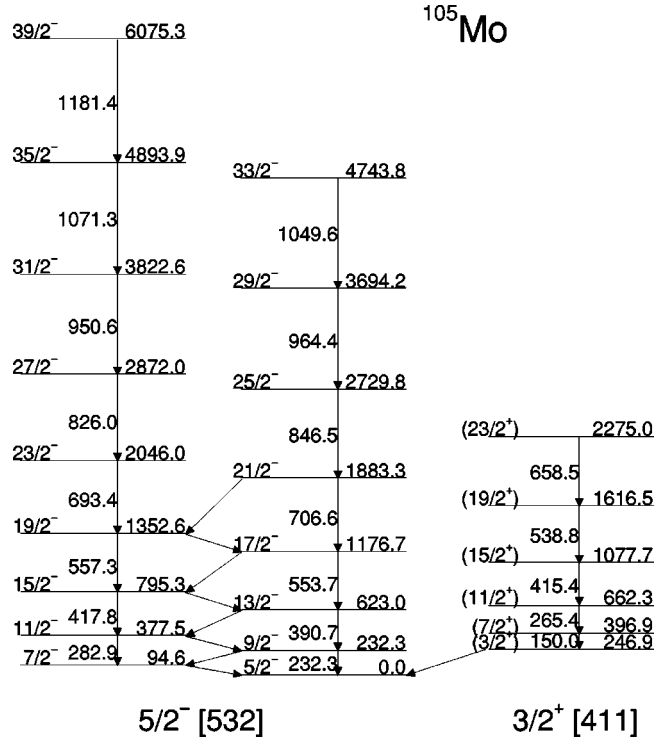

FIG. 16. Partial level scheme of ^{105}Mo. Energies are in keV.

IV. SUMMARY

The rotational bands in neutron-rich Zr and Mo isotopes, which were populated by the ^{238}U(α, f) fusion-fission reaction, have been studied systematically. With a thin target, the deexcitation γ rays were detected by Gammasphere in coincidence with the detection of both fission fragments by CHICO. This technique allowed Doppler-shift corrections to be applied for the observed γ rays. Via such methods, the level schemes of neutron-rich Zr and Mo isotopes have been extended substantially both in spin and excitation energy, and beyond the first band crossing region. The newly acquired knowledge from the odd Zr and Mo isotopes makes it possible to identify the quasiparticle configuration responsible for the observed band crossing. The blocking effects for the $\nu h_{11/2}$ bands in the odd Zr and Mo isotopes indicate that the $h_{11/2}$ neutron alignment is responsible for the first band crossings in the even Zr and Mo isotopes, which is consistent with the prediction of the cranked shell model calculations. The deformed subshell closure at $N=64$ is manifest by the delayed band crossing for the aligned $h_{11/2}$ neutron orbitals in ^{106}Mo. The similarity of the observed J_2 moment between ^{102}Mo and ^{104}Mo indicates that the spin-alignment rate and crossing frequency are insensitive to the softness of the shape degrees of freedom. Study of the high-spin state be-

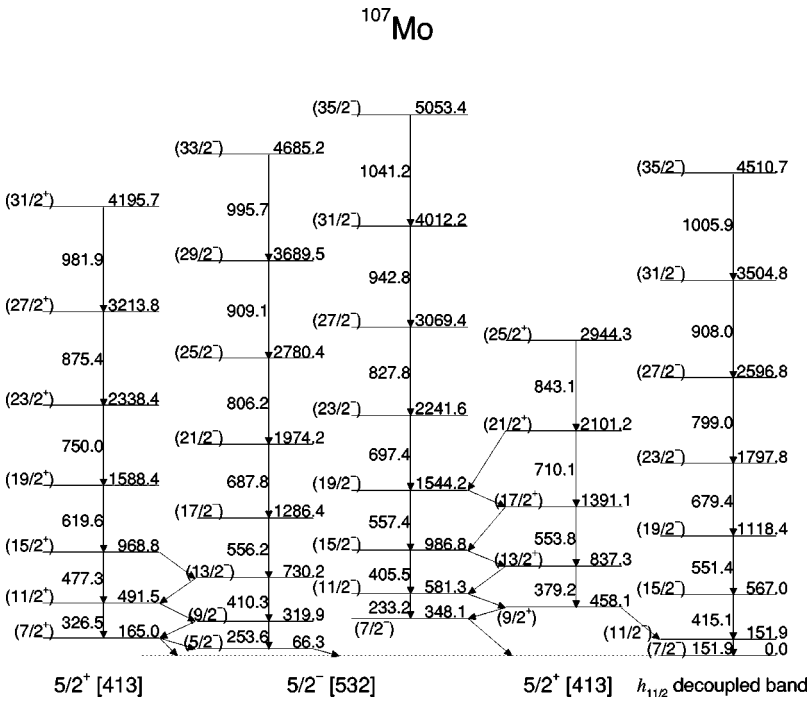

FIG. 17. Partial level scheme of ^{107}Mo. Energies are in keV.

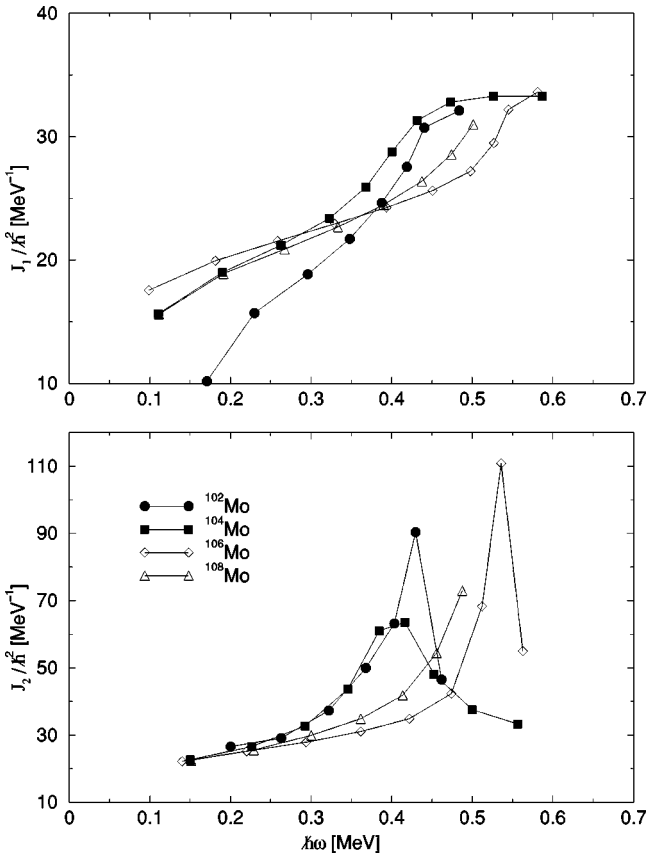

FIG. 18. The kinematic (top) and dynamic (bottom) moments of inertia as a function of the rotational frequency for the ground-state bands in ^{102,104,106,108}Mo.

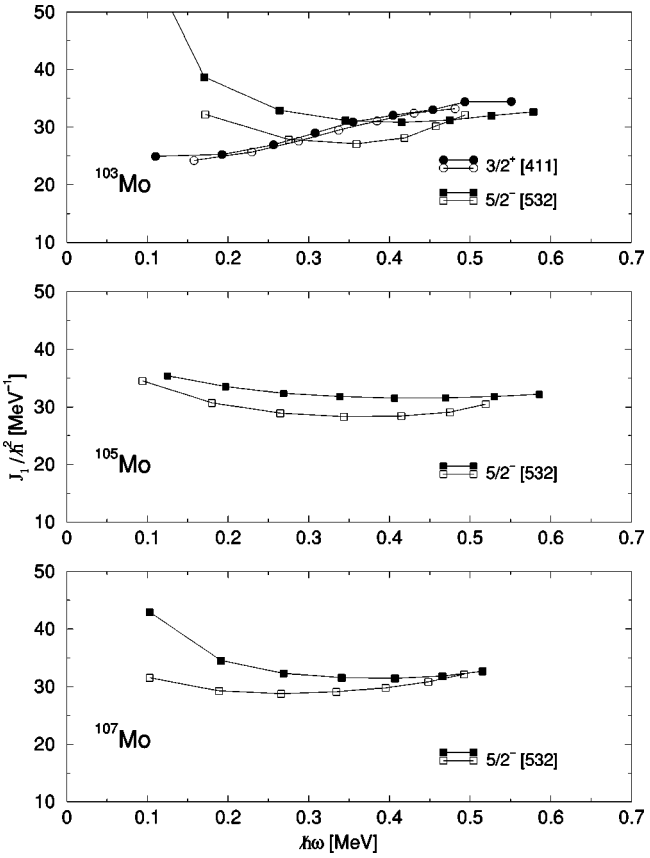

FIG. 19. The kinematic moment of inertia as a function of the rotational frequency for the rotational bands in ^{103}Mo (top), ^{105}Mo (middle), and ^{107}Mo (bottom).

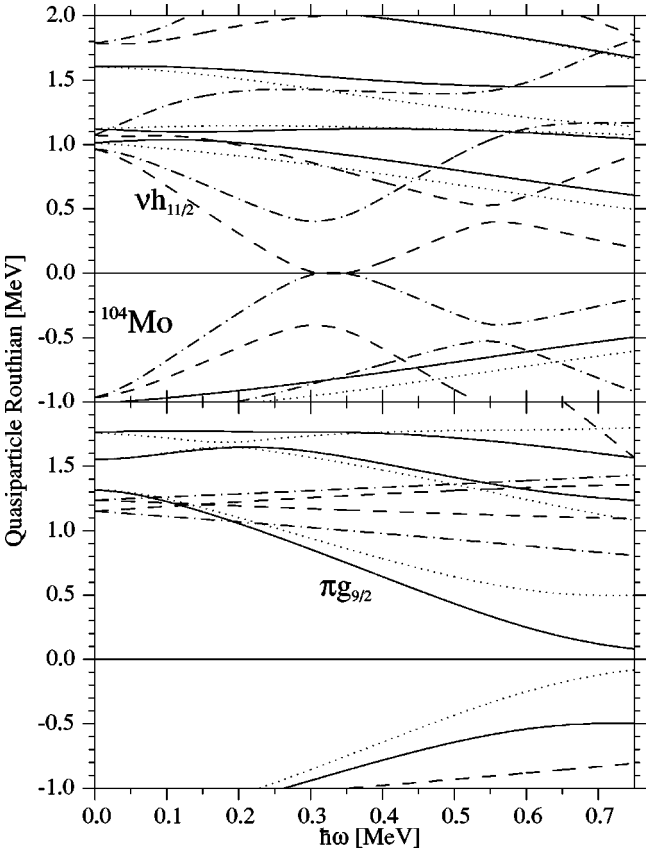

FIG. 20. Cranked shell model calculations for ^{104}Mo. (π, α): solid =(+, +1/2), dotted=(+, −1/2), dash-dotted =(−, +1/2), and dashed =(−, −1/2). The parameters used were β_2=0.33, β_4=0.00, γ=−19°.

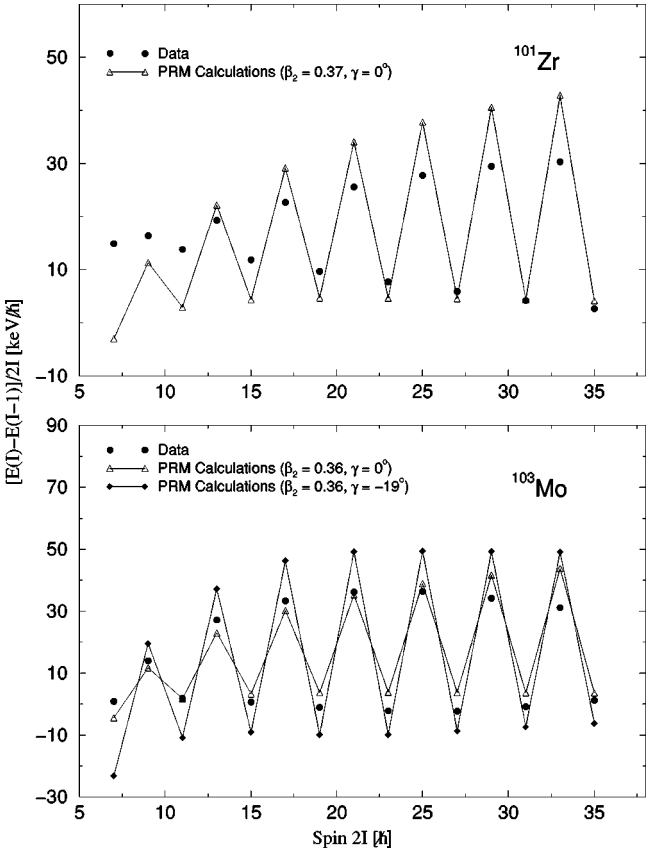

FIG. 21. Experimental and calculated signature splitting for the $\nu h_{11/2}$ bands as a function of spin in ^{101}Zr (top) and ^{103}Mo (bottom).

havior of $5/2^-[532]$ bands in the odd Zr and Mo isotopes using the particle-rotor model implies that the triaxial degree of freedom plays an important role in Mo isotopes while the Zr isotopes still have a more axially symmetry shape. Further experimental and theoretical study of the high-spin states in neighboring nuclei, particularly those having odd-Z numbers, are in progress and will enhance our understanding of nuclear structure for the neutron-rich $A \sim 100$ nuclei.

ACKNOWLEDGMENTS

We would like to acknowledge useful discussions with S. Frauendorf, J. Y. Zhang, and R. A. Wyss. The work by the Rochester group was funded by the National Science Foundation. The work at LBNL was supported in part by the U.S. Department of Energy under Contract No. DE-AC03-76SF00098.

[1] P. Moller, J. R. Nix, W. D. Myers, and W. J. Swiatecki, At. Data Nucl. Data Tables **59**, 185 (1995).
[2] J. Skalski, S. Mizutori, and W. Nazarewicz, Nucl. Phys. **A617**, 282 (1997).
[3] G. A. Lalazissis, S. Raman, and P. Ring, At. Data Nucl. Data Tables **71**, 1 (1999).
[4] H. R. Bowman, S. G. Thompson, and J. O. Rasmussen, Phys. Rev. Lett. **12**, 195 (1964).
[5] E. Cheifetz, R. C. Thompson, and J. B. Wilhelmy, Phys. Rev. Lett. **25**, 38 (1970).
[6] G. Lhersonneau *et al.*, in *Proceedings of the International Conference on the Spectroscopy of Heavy Nuclei*, edited by J. F. Sharpey-Schafer, IOP Conf. Proc. No. 105 (Institute of Physics Publishing, Bristol, 1990), p. 433.
[7] J. H. Hamilton, A. V. Ramayya, S. J. Zhu, G. M. Ter-akopian, Yu. Ts. Oganessian, J. D. Cole, J. O. Rasmussen, and M. A. Stoyer, Prog. Part. Nucl. Phys. **35**, 635 (1995).
[8] F. Schussler, J. A. Pinston, E. Monnand, A. Moussa, G. Jung, E. Koglin, B. Pfeiffer, R. V.F. Janssens, and J. Vanklinken, Nucl. Phys. **A339**, 415 (1980).
[9] K. Becker, G. Jung, K. H. Kobras, H. Wollnik, and B. Pfeiffer, Z. Phys. A **319**, 193 (1984).
[10] H. Mach, M. Moszyński, R. L. Gill, F. K. Wohn, J. A. Winger, John C. Hill, G. Molnàr, and K. Sistemich, Phys. Lett. B **230**, 21 (1989).
[11] K. Shizuma, H. Lawin, and K. Sistemich, Z. Phys. A **311**, 71

(1983).
[12] M. Sambataro and G. Molnàr, Nucl. Phys. **A376**, 201 (1982).
[13] A. G. Smith, J. L. Durell, W. R. Phillips, M. A. Jones, M. Leddy, W. Urban, B. J. Varley, I. Ahmad, L. R. Morss, M. Bentaleb, A. Guessous, E. Lubkiewicz, N. Schulz, and R. Wyss, Phys. Rev. Lett. **77**, 1711 (1996).
[14] A. Guessous, N. Schulz, W. R. Phillips, I. Ahmad, M. Bentaleb, J. L. Durell, M. A. Jones, M. Leddy, E. Lubkiewicz, L. R. Morss, R. Piepenbring, A. G. Smith, W. Urban, and B. J. Varley, Phys. Rev. Lett. **75**, 2280 (1995).
[15] A. Guessous, N. Schulz, M. Bentaleb, E. Lubkiewicz, J. L. Durell, C. J. Pearson, W. R. Phillips, J. A. Shannon, W. Urban, B. J. Varley, I. Ahmad, C. J. Lister, L. R. Morss, K. L. Nash, C. W. Williams, and S. Khazrouni, Phys. Rev. C **53**, 1191 (1996).
[16] M. W. Simon *et al.*, in *Proceedings of the International Conference on Fission and Properties of Neutron Rich Nuclei, Sanibel Island, FL*, edited by J. H. Hamilton and A. V. Ramayya (World Scientific, Singapore, 1998), p. 270.
[17] M. W. Simon, Ph.D thesis, University of Rochester, 1999.
[18] H. Hua, C. Y. Wu, D. Cline, A. B. Hayes, R. Teng, R. M. Clark, P. Fallon, A. Goergen, A. O. Macchiavelli, and K. Vetter, Phys. Lett. B **562**, 201 (2003).
[19] R. Wyss, lecture delivered at the Hands on Nuclear Structure Theory Workshop, Oak Ridge, Tennessee, 1991 (unpublished).
[20] J. Meyer-ter-Vehn, Nucl. Phys. **A249**, 141 (1975).
[21] S. E. Larsson, G. Leander, and I. Ragnarsson, Nucl. Phys. **A307**, 189 (1978).
[22] P. Semmes, lecture delivered at the Hands on Nuclear Structure Theory Workshop, Oak Ridge, Tennessee, 1991 (unpublished).
[23] H. Hua, C. Y. Wu, D. Cline, A. B. Hayes, R. Teng, R. M. Clark, P. Fallon, A. O. Macchiavelli, and K. Vetter, Phys. Rev. C **65**, 064325 (2002).
[24] C. Y. Wu, H. Hua, D. Cline, A. B. Hayes, R. Teng, R. M. Clark, P. Fallon, A. O. Macchiavelli, and K. Vetter, in *Proceedings of the International Conference on Frontiers of Nuclear Structure, Berkeley, CA*, edited by P. Fallon and R. Clark (American Institute of Physics, New York, 2002), p. 408.
[25] C. Y. Wu, H. Hua, D. Cline, A. B. Hayes, R. Teng, R. M. Clark, P. Fallon, A. O. Macchiavelli, and K. Vetter, *Proceedings of the Third International Conference on Fission and Properties of Neutron-Rich Nuclei, Sanibel Island, FL*, edited by J. H. Hamilton, A. V. Ramayya, and H. K. Carter (World Scientific, Singapore, 2003), p. 199.
[26] M. W. Simon, D. Cline, C. Y. Wu, R. W. Gray, R. Teng, and C. Long, Nucl. Instrum. Methods Phys. Res. A **452**, 205 (2000).
[27] J. Weber, H. Specht, E. Konechy, and D. Heunemann, Nucl. Phys. **A221**, 414 (1974).
[28] C. Y. Wu, M. W. Simon, D. Cline, G. A. Davis, A. O. Macchiavelli, and K. Vetter, Phys. Rev. C **57**, 3466 (1998).
[29] K. Vetter, A. O. Macchiavelli, D. Cline, H. Amro, S. J. Asztalos, B. C. Busse, R. M. Clark, M. A. Deleplanque, R. M. Diamond, P. Fallon, R. Gray, R. V.F. Janssens, R. Krucken, I. Y. Lee, R. W. MacLeod, E. F. Moore, G. J. Schmid, M. W. Simon, F. S. Stephens, and C. Y. Wu, Phys. Rev. C **58**, 2631 (1998).
[30] C. Y. Wu, D. Cline, M. W. Simon, R. Teng, K. Vetter, M. P. Carpenter, R. V.F. Janssens, and I. Wiedenhover, Phys. Rev. C **61**, 021305(R) (2000).
[31] C. Y. Wu, M. W. Simon, D. Cline, G. A. Davis, R. Teng, A. O. Macchiavelli, and K. Vetter, Phys. Rev. C **64**, 064317 (2001).
[32] M. A.C. Hotchkis, J. L. Durell, J. B. Fitzgerald, A. S. Mowbray, W. R. Phillips, I. Ahmad, M. O. Carpenter, R. V.F. Janssens, T. L. Khoo, E. F. Moore, L. R. Morss, P. Benet, and D. Ye, Nucl. Phys. **A530**, 111 (1991).
[33] R. C. Jared, H. Nifenecker, and S. G. Thompson, *Proceedings of the Third Symposium on Physics and Chemistry of Fission, IAEA Rochester, New York* (IAEA-SM-174, Vienna, 1974), Vol. II, p. 211.
[34] J. L. Durell, Bull. Am. Phys. Soc. **38**(9), 1794 (1993).
[35] J. L. Durell, W. R. Phillips, C. J. Pearson, J. A. Shannon, W. Urban, B. J. Varley, N. Rowley, K. Jain, I. Ahmad, C. J. Lister, L. R. Morss, K. L. Nash, C. W. Williams, N. Schulz, E. Lubkiewicz, and M. Bentaleb, Phys. Rev. C **52**, 2306 (1995).
[36] J. H. Hamilton, Q. H. Lu, S. J. Zhu, K. Bulter-Moore, A. V. Ramayya, B. R.S. Babu, L. K. Peker, W. C. Ma, T. N. Ginter, J. Kormicki, D. Shi, J. K. Deng, J. O. Rasmussen, M. A. Stoyer, S. Y. Chu, K. E. Gregorich, M. F. Mohar, S. Prussin, J. D. Cole, R. Aryaeinejad, N. R. Johnson, I. Y. Lee, F. K. McGowan, G. M. Ter-Akopian, and Yu. Ts. Oganessian, in *Proceedings of the International Conference on Exotic Nuclei and Atomic Masses, Arles, France*, edited by M. de Saint Simon and O. Sorlin (Editions Frontieres, Gif-sur-Yvette, 1995), p. 487.
[37] W. Urban, J. A. Pinston, T. Rzaca-Urban, A. Zlomaniec, G. Simpson, J. L. Durell, W. R. Phillips, A. G. Smith, B. J. Varley, I. Ahmad, and N. Schulz, Eur. Phys. J. A **16**, 11 (2003).
[38] R. B. Firestone, V. S. Shirley, C. M. Baglin, S. Y.F. Chu, and J. Zipkin, *Table of Isotopes*, 8th ed. (Wiley, New York, 1996), Vol. I.
[39] G. Lhersonneau, P. Dendooven, A. Honkanen, M. Huhta, M. Oinonen, H. Penttila, J. Aysto, J. Kurpeta, J. R. Persson, and A. Popov, Phys. Rev. C **54**, 1592 (1996).
[40] M. Liang, H. Ohm, B. Desutterpomme, and K. Sistemich, Z. Phys. A **351**, 13 (1995).
[41] J. K. Hwang, A. V. Ramayya, J. H. Hamilton, L. K. Peker, J. Kormicki, B. R.S. Babu, T. N. Ginter, G. M. TerAkopian, Y. T. Oganessian, A. V. Daniel, W. C. Ma, P. G. Varmette, J. O. Rasmussen, S. J. Asztalos, S. Y. Chu, K. E. Gregorich, A. O. Macchiavelli, R. W. Macleod, J. Gilat, J. D. Cole, R. Aryaeinejad, K. ButlerMoore, M. W. Drigert, M. A. Stoyer, Y. X. Dardenne, J. A. Becker, L. A. Bernstein, R. W. Lougheed, K. J. Moody, S. G. Prussin, H. C. Griffin, and R. Donangelo, Phys. Rev. C **56**, 1344 (1997).
[42] M. Liang, H. Ohm, B. De Sutter, K. Sistemich, B. Fazekas, and G. Molnàr, Z. Phys. A **340**, 223 (1991).
[43] L. M. Yang, S. J. Zhu, K. Li, J. H. Hamilton, A. V. Ramayya, J. K. Hwang, X. Q. Zhang, L. Y. Zhu, C. Y. Gan, M. Sakhaee, G. L. Long, R. Q. Xu, Z. Zhang, Z. Jiang, M. G. Jon, W. C. Ma, B. R.S. Babu, J. Komicki, E. F. Jones, J. D. Cole, R. Aryaeinejad, M. W. Drigert, T. Y. Lee, J. O. Rasmussen, M. A. Stoyer, G. M. Ter-Akopian, and A. V. Daniel, Chin. Phys. Lett. **18**, 24 (2001).
[44] W. R. Phillips, I. Ahmad, H. Emling, R. Holzmann, R. V. F. Janssens, T. L. Khoo, and M. V. Drigert, Phys. Rev. Lett. **57**, 3257 (1986).